Neutron diffraction from small numbers of Langmuir-Blodgett monolayers of manganese stearate

R. M. Nicklow

Solid State Division, Oak Ridge National Laboratory, Oak Ridge, Tennessee 37830

M. Pomerantz and Armin Segmüller

IBM T. J. Watson Research Center, Yorktown Heights, New York 10598

We report the observation of neutron diffraction from as few as three monolayers of manganese stearate on a plate of about 4-cm² area. These room-temperature (paramagnetic state) measurements could be adequately calculated on a laminar model of the crystal structure. Similar calculations, extended to a hypothetical magnetically ordered structure, indicate that the interlayer magnetic structure would be observable already with three layers of magnetic unit cells.

I. INTRODUCTION

The goal of this study was to determine the magnetic structure of the ordered state of magnetic multilayers by neutron diffraction. Many quasi-two-dimensional (2D) magnetic crystals have been investigated.[1] In almost every case, if magnetic ordering occurred it was three-dimensional, implying that the interaction between the magnetic layers was ultimately significant. One wonders if the layers can be spread sufficiently far apart, reducing the coupling such that individual planes only will have magnetic order. There are mean-field theoretical arguments denying this possibility.[2] The reasoning was that as an individual layer approaches T_{2D}, an ordering temperature, its susceptibility diverges. Then any interplanar field, however small, will produce ordering between the planes which sets in slightly below T_{2D}.

We have begun to investigate this question using magnetic monolayers of manganese stearate [Mn $(C_{18}H_{35}O_2)_2$, abbreviated MnSt$_2$]. It has been shown[3] that this compound can be deposited as individual monolayers or as multilayers with spacing between Mn layers of about 50 Å. A monolayer of the material seems to order magnetically[4] below about 2 K to a weak ferromagnetic state. Since the interplanar spacing is more than twice that of any other reported[1] quasi-2D magnet—and could easily be made larger—this seems to be an appropriate material to study weak interlayer interactions.

Such experiments require low temperatures and have not yet been completed. Our results at room temperature, which are the subject of this paper, show that it is possible to successfully observe neutron diffraction from a few monolayers with an area of a few cm². The mass of the sample is ~ 10⁻⁶ g which is probably the smallest to ever give observable neutron diffraction. We will describe calculations of the diffraction pattern which agree well with the experiments, even when large variations are introduced by isotopic substitution. We also present calculations of magnetic diffraction for a particular (optimal) ordered state of the magnetic structure.

The study of artificial multilayers as monochromators and polarizers in neutron diffraction was pioneered by Schoenborn and collaborators.[5] Magnetic effects in multilayers were discussed by Lynn et al.,[6] Mezei,[7] and Sato and Abe.[8] Their films were prepared by evaporation of multilayers of materials of differing neutron cross section. This permitted the optimization of the relative refractive indices to produce large reflections. There were difficulties with uniformity of the thickness of the many layers, and consequently fine details tended to be blurred. We have used the Langmuir-Blodgett technique[9] to deposit multilayers. This restricts the kinds of materials we deposit, but it provides films with precisely repeated spacing of successive layers.

II. EXPERIMENTAL TECHNIQUES

The Langmuir-Blodgett technique is thoroughly reviewed elsewhere.[3,4,9] Basically, it involves the spreading of long-chain fatty acid molecules on the surface of water. Stearic acid was employed in this work. Such molecules float on the surface as a monolayer: the "fatty" hydrophobic end trying to emerge and the "acid" ionic end trying to dissolve in the water. Manganese can be chemically bound to the ionic end in the water, thus forming MnSt$_2$. The monolayer can be removed from the water surface by compressing the layer and then inserting and retracting a substrate (polished Si wafers were used) through the water surface. It was found that a monolayer deposits on each pass through the surface,

except the first, giving an odd number of layers in the film. The fatty ends of the molecules attach to each other, and the ionic (Mn) ends to each other. This gives a bilayer unit cell with a spacing of about two 25 Å chain lengths. The stearic acid ($C_{18}H_{35}OOH$) was purchased from Analabs. Deuterated stearic acid ($C_{18}D_{35}OOH$) was purchased from Merck Sharp and Dohme Canada Limited.

To check the quality of the samples we measured the x-ray diffraction from them. The x-ray small-angle interference data were taken on a computer-controlled diffractometer using highly collimated and highly monochromated Cu $K\alpha_1$ radiation, which has been described thoroughly elsewhere.[10]

The neutron measurements were carried out on the triple-axis neutron spectrometer located at the HB-2 beam hole of the High Flux Isotope Reactor at the Oak Ridge National Laboratory. The (002) planes of a pyrolitic graphite crystal, having a mosaic spread of approximately 0.4°, were used as the monochromator. Because of the large cell spacing (~ 50 Å) of the sample, a relatively long neutron wavelength of 4.15 Å was used in order to better resolve the Bragg reflections. This wavelength also permitted the use of a Be filter to suppress higher-order wavelength contamination ($\lambda/n, n = 2, 3, 4$, etc.) from the monochromator which would have given diffraction peaks from the Si substrate in the same angular range as the peaks from the $MnSt_2$ films. The wavelength of the neutron beam was measured in a separate monochromator calibration experiment carried out with a Ni powder standard. It was remeasured several times during the course of the present experiment by noting the diffraction angle for the (111) planes of the Si substrate of each sample.

The collimation of the incident beam was 20' full width at half maximum (FWHM). No collimation was used after the sample. Several preliminary measurements were carried out with a wide open detector and with a pyrolitic graphite analyzer (or post monochromator) inserted between the sample and the detector. The analyzer had a mosaic spread of approximately 0.8° (FWHM) and it was oriented with the (002) plane set to diffract into the detector 4.15 Å neutrons scattered by the sample. With the analyzer in place the detector did not directly "see" the sample. This resulted in a substantially lower background with no appreciable degradation of the signal or alteration of its angular dependence, thereby giving a significant improvement in the signal-to-background ratio compared to the results obtained with a wide open detector. This spectrometer geometry gave an angular resolution for 2θ of approximately 0.8°, where θ is the glancing angle of the beam with respect to the plane of the film.

The results discussed below were obtained from standard θ-2θ scans (sample and detector stepping in a 1:2 ratio) with the analyzer crystal in place. Due

to the small number of $MnSt_2$ layers in each film real diffracted intensity arising from the subsidiary peaks discussed below exists between the main Bragg peaks. Consequently, the background appropriate to each point in the θ-2θ scan was obtained by rotating only the sample angle θ approximately 2–3° with the detector 2θ fixed. The data shown in Figs. 3,5,6, and 7 have been corrected for the background. Typical counting times were 10 to 20 min per point.

III. EXPERIMENTAL RESULTS

It had earlier been shown[10] that x-ray diffraction from $MnSt_2$ films could be observed and quantitatively explained down to even a single monolayer. An illustration of this is given in Fig. 1 where the x-ray diffraction from a 43-layer film prepared for this study is shown by the points. The solid curve is the result of a calculation using the parameters determined from the earlier study[10] of films consisting of from 1 to 11 layers. The fit is so good that the calculated curve was displaced downward to avoid obscuring the data points. Note that the stearate chain was totally deuterated in this sample but this had no noticeable effect on the quality of the fit, i.e., to our accuracy the pertinent x-ray parameters are unchanged by deuteration.

It was pointed out[3,10,11] that because of the finite number of layers the diffraction had, in addition to
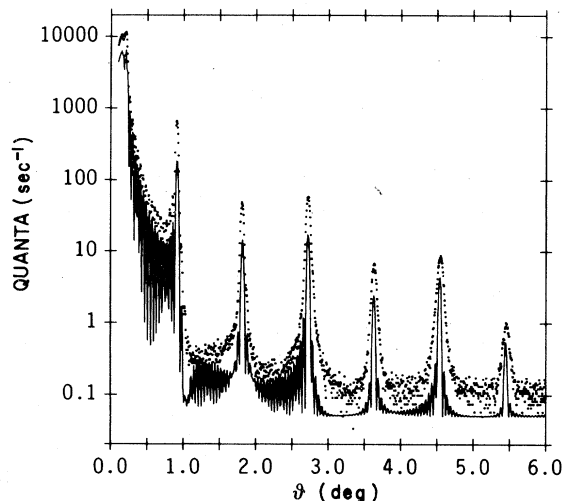
FIG. 1. X-ray diffraction from a film of 43 layers of per-deuterated manganese stearate on a Si substrate. Experimental values shown as points. The solid curve is a calculation based on a model laminar structure, whose refractive indices and thicknesses were obtained in Ref. 10 and are listed under δ_x and THICK (X, H, and D) in Fig. 4. The calculation was displaced from the data points to avoid obscuring them. θ = grazing angle and the x-ray wavelength = 1.54 Å.

the Bragg peaks, subsidiary maxima which could be unusually large for Langmuir-Blodgett multilayers. By analogy with optical diffraction gratings with N slits, where there are $N-2$ subsidiary diffraction maxima, one expects for a sample of $\mathcal{L}$ layers the number of x-ray subsidiary maxima to be $\approx (\mathcal{L}/2) - 2$ since there are $(\mathcal{L}-1)/2$ unit cells in the normal direction. This was observed in the 43-layer sample; the experimental results in the angular region between the grazing angle $\theta = 0$ and $1°$ are shown in Fig. 2. The high resolution of the x-ray measurement allows at least 16 subsidiary peaks to be identified. The solid curve was computed on the multilayer model with small changes in the parameters used in Fig. 1 and Ref. 10. We exhibit this to emphasize the precise regularity of the layer spacing which the Langmuir-Blodgett method provides.

The same sample produces the neutron diffraction pattern shown by the dots in Fig. 3. The neutron wavelength was 4.15 Å. We calculated the neutron diffraction by the same method used for the x-ray diffraction, as given in detail in Ref. 10. This method treats each layer as a series of laminae corresponding to the chemically different parts of the molecules, as illustrated in Fig. 4. Each lamina is characterized by its thickness and a complex refractive index, n, which depends on its chemical composition

$$n = 1 - \delta - i\beta \ . \tag{1}$$

For x rays[12]

$$\delta_x = r_e Z N \lambda_x^2/2\pi \ , \tag{2}$$

where $r_e = e^2/mc^2 = 2.8 \times 10^{-13}$ cm = classical electron radius, Z = atomic number, and N = density of
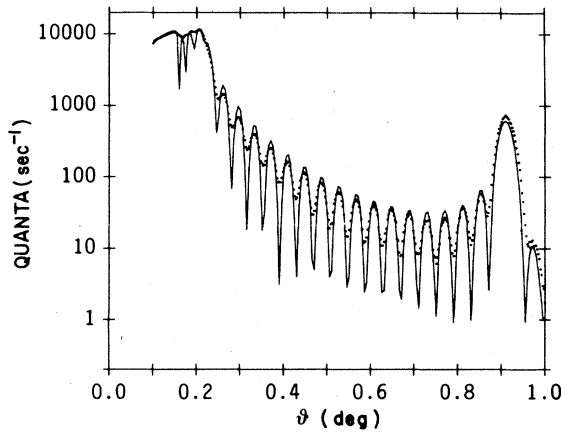
FIG. 2. The data of Fig. 1 in the region $\theta = 0$ to $1°$. The calculation of diffraction (solid curve) used optimized parameters obtained by the simplex method, but which did not differ much from those used in Fig. 1.
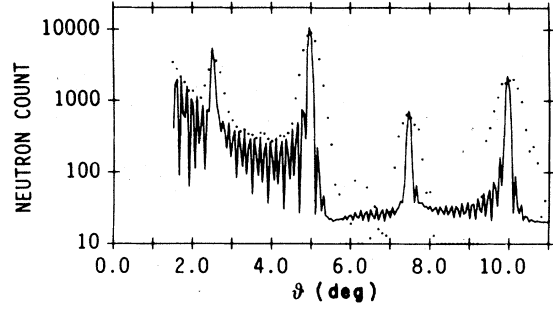
FIG. 3. Neutron diffraction from the same film as in Fig. 1 (the dots). The calculation (solid curve) was made on the laminar model using the parameters $\delta_n^n(D)$, THICK (n, D) listed in Fig. 4. These were obtained by a simplex optimization using as starting values δ_n^x for D–C–D and D layers and THICK $(X, H,$ and $D)$. Neutron wavelength = 4.15 Å.

atoms. β can be obtained from measured absorption coefficients, μ_x,[13] by $\beta_x = \mu_x \lambda_x/4\pi$. One then treats the film as a multilayer dielectric in order to calculate its reflection and interference behavior.

Similar concepts apply to neutron diffraction. The real part of the refractive index, is[14]

$$\delta_n = \bar{b} N \lambda_n^2/2\pi \ , \tag{3}$$

where $\bar{b}$ is the coherent scattering amplitude. The imaginary part of n can be expressed in terms of the neutron absorption coefficient. In order to determine the values of δ and β, we started by simply scaling from our best values[10] for δ_x, using the ratio of Eqs. (2) and (3):

$$\delta_n = \delta_x (\bar{b} \lambda_n^2/r_e Z \lambda_x^2) \tag{4}$$

and similarly for β. We found that for reasonable values of β the results were independent of β. Thus, we set all $\beta = 0$ in the calculations: absorption has no effect. Using tabulated[14] values of $\bar{b}$ for the elements, we obtained the values denoted by δ_n^x in Fig. 4. Note that they are of similar magnitude as δ_x so that, relative to the incident flux, diffraction intensities can be expected to be similar for neutrons and x rays. These δ_n^x and thicknesses from x-ray measurements (denoted by THICK X, H, and D) were initial values for a fitting of the data by varying δ's and thicknesses to obtain a best fit using the simplex method.[15] The optimizing δ's and thicknesses are listed in Fig. 4 under $\delta_n^n(D)$ and THICK (n, D). They are fairly close to the initial estimates. The resulting computed diffraction is shown by the solid line in Fig. 3. It has narrower peaks than those observed, in agreement with our estimate of resolution of about $0.4°$ in θ. This also explains why no subsidiary maxima are resolved at low angles.

A feature present in neutron diffraction is that isotopic substitution can change the refractive index, be-

Layer	Material	δ_x (/10^{-6})	δ_n^x (/10^{-6})	$\delta_n^n(H)$ (/10^{-6})	$\delta_n^n(D)$ (/10^{-6})	THICK (X,H&D)	THICK (n,H)	THICK (n,D)
3rd LAYER		11.6	9.6	7.0	9.8	0	0.72	1.1
	Mn	5.95	-2.4	-3.0	-2.4	0	0.19	0.02
		11.90	-4.8	-6.0	-4.8	1.16	0.42	0.50
	Mn	5.95	-2.4	-3.0	-2.4	0	0.19	0.02
		11.6	9.6	7.0	9.8	0	0.72	1.1
	COO	5.65	12.1	10.0	12.2	2.08	1.9	1.4
2nd LAYER	H-C-H or D-C-D	3.6	-0.99 or 23.8	-0.30	21.2	20.9	19.8	20.1
	H or D	0.7	-6.8 or 12.1	-4.3	9.5	1.6	2.4	2.2
1st LAYER	H-C-H or D-C-D	3.9	-1.07 or 25.7	-1.5	21.2	20.0	19.8	20.1
	COO	5.9	12.6	10.6	12.2	2.08	1.88	1.4
		12.1	10.1	7.7	9.8	0	0.72	1.1
	Mn	6.2	-2.5	-2.8	-2.4	1.2	0.61	0.52
	SiO	8.1	11.3	6.6	6.6	25	15.9	9.2
SUB-STRATE	Si	7.6	5.9	6.4	6.4	∞	∞	∞

FIG. 4. Schematic of the laminar model used to calculate x-ray and neutron diffraction from $MnSt_2$ multilayers (not to scale). This model is described in more detail in Ref. 10, wherein the x-ray parameters δ_x, THICK (X, H, and D) were determined. The neutron parameters are explained in the text and in the captions of Figs. 3 and 5.

cause the scattering length, $\bar{b}$, is a nuclear property. Thus, unlike the x-ray result on a deuterated sample (Fig. 1) which could be fitted with the δ obtained from a protonated sample, the neutron diffraction is dramatically different in protonated versus deuterated samples. The neutron diffraction from a 37-layer film of (protonated) $MnSt_2$ is shown in Fig. 5. A major difference between this result and that on the deuterated sample is that the diffraction peaks decrease monotonically, whereas they alternated in intensity in the deuterated sample. The calculation of the diffraction reproduces these observations when account is taken of the large difference between the scattering length of deuterons, $(\bar{b} = 0.667 \times 10^{-12}$ cm) and protons $(\bar{b} = -0.374 \times 10^{-12}$ cm). The starting and optimum values for the calculation on the protonated sample are listed under δ_n^x, THICK (X, H, and D), $\delta_n^n(H)$, and THICK (n, H), respectively. Again,
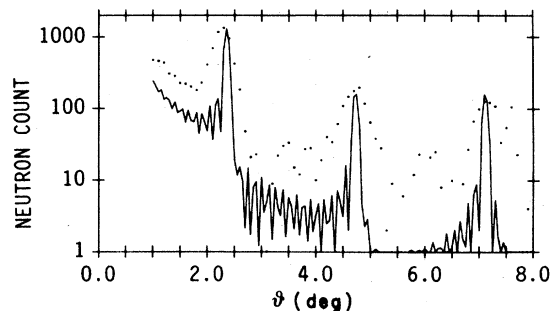
FIG. 5. Neutron scattering from a 37-layer film of (protonated) $MnSt_2$, indicated by the dots. The solid curve is calculated from the laminar model shown in Fig. 4. Optimized parameters $\delta_n^n(H)$ and THICK (n, H) were obtained by the simplex method, with initial values δ_n^x (for H–C–H and H layers) and THICK (X, H, and D) as listed in Fig. 4.

the agreement of the computed curve with the data points in Fig. 5 is fairly good. The discrepancies may arise from not taking account of the resolution, which is difficult.

An interesting difference between the x-ray and neutron diffraction parameters is that the optimum thicknesses for the neutron diffraction indicate some overlap of the Mn with the COO group, and some regions where the Mn of one layer does not overlap the Mn in the next. (cf. Fig. 4.) The x-ray parameters were optimum for complete overlap of the Mn with each other, and no overlap with COO. Not too much confidence can be placed in this rather fine detail, considering that the fits to the neutron data are not as good as to the x-ray data.

The problem with the instrumental resolution can be ameliorated by measuring samples with smaller numbers of layers. The true width of the diffraction peaks and subsidiaries increases and can then be greater than the experimental resolution. This is illustrated in Fig. 6, for a sample of 11 layers of perdeuterated $MnSt_2$. The computed and observed peaks have about the same width. Comparing with Fig. 3, we identify the peak near $\theta = 2.5°$ as the (001) Bragg peak. The predicted subsidiary peaks, the solid lines, may be barely visible. The optimizing parameters, δ and thicknesses, are generally close to those found for the 43-layer sample as listed in Fig. 4. The largest difference is δ for the D−C−D lamina which was 25.1×10^{-6} for the 11-layer sample instead of 21.2×10^{-6} for the 43-layer sample. The calculations indicate overlap of the Mn and COO, similar to that described above.

As a final experimental result we show in Fig. 7 the experimental and calculated diffraction from 3 layers of perdeuterated $MnSt_2$. The optimizing parameters δ differ even more from those listed in Fig. 4. We find δ (D−C−D) $= 29.0 \times 10^{-6}$ and δ (COO) $= 15.0 \times 10^{-6}$, for example. But the accuracy of these values is limited by the weakness of the signal. Thus, the accuracy is limited for small numbers
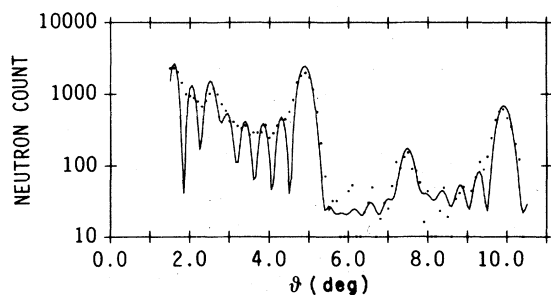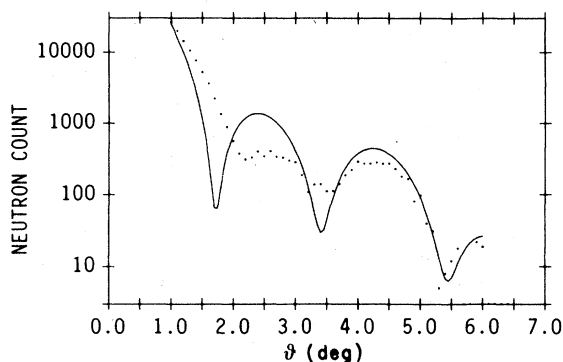
FIG. 7. Same as Fig. 6 except the film is 3 layers of perdeuterated $MnSt_2$.

of layers by the small intensities and for large numbers of layers by resolution. Nevertheless, there is semiquantitative agreement of experiment and calculation even down to three monolayers, on a 4 cm^2 substrate. This has a total sample weight of about 3×10^{-6} g, probably the smallest amount that has ever given an observable neutron diffraction pattern.

IV. CALCULATION OF DIFFRACTION FROM MAGNETICALLY ORDERED LAYERS

The previous section showed that neutron diffraction is observable from modest areas and small numbers of Langmuir-Blodgett layers of $MnSt_2$. It was also seen that the calculation of the diffraction using a model of a multilamina representation of each layer gave reasonably good agreement with the data, using known neutron scattering lengths. This encourages us to predict the diffraction from magnetically ordered structures.

The magnetic structure of $MnSt_2$ monolayers appears[4] to be antiferromagnetic in each layer, with a weak ferromagnetic component. The ordering of these antiferromagnetic planes with respect to each other would be difficult to observe because each plane has only a very small magnetic moment. By this method of low angle diffraction we can observe only the ordering between planes, not ordering within a plane. Thus we feel it is unlikely, unless our understanding of the ordering in $MnSt_2$ is wrong, that we will observe the interplane ordering.

As an exercise, however, let us consider the conditions for observing the most favorable case of interplane ordering. It is well known[14] that neutron scattering from magnetically ordered media is proportional to $\vec{q} = \vec{\epsilon} (\vec{\epsilon} \cdot \vec{K}) - \vec{K}$, where $\vec{\epsilon}$ is a unit normal to the reflecting plane and $\vec{K}$ is a unit vector parallel to the atomic magnet moment. The magnitude of $|q| = \sin\alpha$ where α is the angle between $\vec{\epsilon}$

FIG. 6. Neutron scattering from an 11-layer film of perdeuterated $MnSt_2$ (dots). The solid curve was calculated on the laminar model of Fig. 4 with parameters optimized for this case. They differed slightly from those listed in Fig. 4.
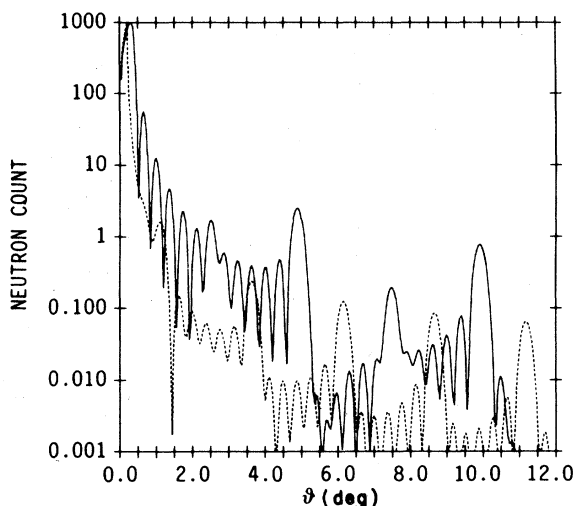
FIG. 8. Computed neutron scattering from a hypothetical ordered magnet of $MnSt_2$. Diffraction from the nuclei of a 13-layer film of perdeuterated $MnSt_2$ is given by the solid curve. The dotted curve is the magnetic scattering from ferromagnetic layers of Mn^{2+} ions where successive layers are antiferromagnetically aligned.

FIG. 9. Same as Fig. 8, except protonated $MnSt_2$ is taken. This changes the nuclear scattering which makes some magnetic peaks more discernible.

and $\vec{K}$. The maximum $|q|$, and scattering, is thus when $\vec{\tau}$ and $\vec{K}$ are perpendicular, i.e., the atomic moments lie in the reflecting planes. It is also easiest to detect antiferromagnetic ordering because this gives rise to new peaks between the nuclear Bragg peaks.[14] Thus, the model we calculated was Mn atoms ferromagnetically aligned, with moments lying in the planes, and alternate planes antiferromagnetically aligned. Such a magnetic structure is experimentally observed in some layered copper compounds,[1,16] but for consistency we continue to consider Mn layers. The magnetic scattering amplitude of Mn^{2+} is[14] $p = 1.35 \times 10^{-12}$ cm. The value of $\delta_n = \pm 17.1 \times 10^{-6}$ for the magnetic scattering was found by scaling from the nuclear $\bar{b}$.

The curves of Figs. 8 and 9 show the calculated nuclear diffraction as the solid lines and the calculated magnetic diffraction as the dotted lines. Both calculations were for films of 13 layers of $MnSt_2$ which is, thus, $6\frac{1}{2}$ lattice unit cells and $3\frac{1}{4}$ magnetic unit cells thick. In Fig. 8, the lattice diffraction was computed for perdeuterated stearate, and of course it closely resembles the diffraction measured in the 11-layer film shown in Fig. 6. The magnetic diffraction peak near $\theta = 6.2°$ is predicted to be of comparable amplitude to the lattice diffraction peak at about 7.5°, which is readily observable in Fig. 6. Thus, we conclude that magnetic diffraction could be observed in such a sample of as few as three magnetic unit cells in thickness.

The calculation of diffraction from a protonated

sample, shown in Fig. 9, again predicts that the antiferromagnetic peaks are of comparable magnitude to the nuclear peaks. In fact the magnetic peak at $\theta = 3.7°$ should be observable in this case because the subsidiary nuclear peaks at this angle are weaker than in the deuterated sample, and will not overwhelm the magnetic peak.

V. SUMMARY AND CONCLUSIONS

We have observed neutron diffraction from as few as three monolayers of $MnSt_2$ on a 4-cm^2 plate. This unusually high sensitivity arises[10] because the Bragg peaks are at low angles, as a consequence of the large size of the unit cell (~ 50 Å) in the normal direction. The Bragg angles are close enough to the angle of total reflection that the intensity of the reflected neutron beam is high, and the interference effects are pronounced.

The diffraction can be well calculated using a model structure: laminae corresponding to each chemical constituent of the molecule. The refractive properties of each layer could be approximately obtained from previous x-ray measurements and known values of the neutron scattering lengths. Fitting to the data gave values of thicknesses and refractive indices that differed from the starting estimates by less than 20% for the important parameters. The neutron results indicated some overlap of the Mn with the COO group which was not found in the x-ray study. These are fine details that are probably outside of the accuracy of our work.

The particular advantage of neutron diffraction is

in determining magnetic structures. Such measurements are in preparation. It seems unlikely that they will be fruitful for the case of $MnSt_2$ because it appears to be mostly antiferromagnetic in each plane; there will be little scattering from such a plane. There might be a reduction in the incoherent (paramagnetic) scattering which could identify the magnetic transition.

To illustrate the possibilities of magnetic neutron diffraction from a small number of layers we calculated the diffraction from multilayers of Mn separated by about 50 Å. The Mn were assumed to be in planes with ferromagnetic alignment within the planes, and antiferromagnetic alignment of successive planes. The calculations indicate that in this optimum case antiferromagnetic peaks should be observable for about 13 or more deposited layers, i.e., about three magnetic unit cells.

ACKNOWLEDGMENTS

[1]L. J. de Jongh and A. R. Miedema, Adv. Phys. **23**, 1 (1974).

[2]Y. Imry, Phys. Rev. B **13**, 3018 (1976).

[3]M. Pomerantz, A. Segmüller, and F. Dacol, Phys. Rev. Lett. **40**, 246 (1978).

[4]M. Pomerantz, Solid State Commun. **27**, 1413 (1978); and in *Phase Transitions in Surface Films,* edited by J. G. Dash and J. Ruvalds (Plenum, New York, 1980), p. 317.

[5]B. P. Schoenborn, D. L. D. Caspar, and O. F. Kammer, J. Appl. Phys. **7**, 508 (1974).

[6]J. W. Lynn, J. K. Kjems, L. Passell, A. M. Saxena, and B. P. Schoenborn, Acta Crystallogr. **9**, 454 (1976).

[7]F. Mezei, Comments Phys. **1**, 81 (1976).

[8]M. Sato and K. Abe, Solid State Commun. **26**, 95 (1978).

[9]G. L. Gaines, *Insoluble Monolayers at Liquid-Gas Interfaces* (Interscience, New York, 1966), reviews the technique.

[10]M. Pomerantz and A. Segmüller, Thin Solid Films **68**, 33 (1980).

[11]D. C. Bisset and J. Iball, Proc. Phys. Soc. London Sect. A **67**, 315 (1954).

[12]R. W. James, *The Optical Principles of the Diffraction of X-Rays* (Bell, London, 1950), p. 167.

[13]*International Tables for X-Ray Crystallography* (Kynoch, Birmingham, 1962).

[14]G. E. Bacon, *Neutron Diffraction* (Clarendon, Oxford, 1975).

[15]A. Segmüller, in *Modulated Structures—1979,* edited by J. M. Cowley, J. B. Cohen, M. B. Salamon, and B. J. Wuensch, AIP Conf. Proc. No. 53 (AIP, New York, 1979), p. 78.

[16]P. Bloembergen, Physica (Utrecht) **79B**, 467 (1975).